Dopaminergic Pathways and Resting-state Functional Connectivity in Parkinson's Disease with Freezing of Gait

Kenan Steidel[1§], Marina C. Ruppert[1,2§], Irina Palaghia[1], Andrea Greuel[1], Masoud Tahmasian[3,4], Franziska Maier[5], Jochen Hammes[6], Thilo van Eimeren[6,7,10], Lars Timmermann[1,2], Marc Tittgemeyer[8,9], Alexander Drzezga[6,10,11], David Pedrosa[1,2], Carsten Eggers[1,2]

§= the authors contributed equally to this work

[1] *Department of Neurology, University Hospital of Marburg, Germany*

[2] *Center for Mind, Brain and Behavior - CMBB, Universities Marburg and Gießen, Germany*

[3] *Institute of Systems Neuroscience, Medical Faculty, Heinrich Heine University Düsseldorf, Düsseldorf, Germany.*

[4] *Institute of Neuroscience and Medicine, Brain & Behaviour (INM-7), Research Centre Jülich, Jülich, Germany*

[5] *Department of Psychiatry, University Hospital Cologne, Medical Faculty, Cologne, Germany*

[6] *Multimodal Neuroimaging Group, Department of Nuclear Medicine, Medical Faculty and University Hospital Cologne,*

University Hospital Cologne, Germany

[7] *Department of Neurology, Medical Faculty and University Hospital Cologne, University Hospital Cologne, Germany*

[8] *Max Planck Institute for Metabolism Research, Cologne, Germany*

[9] *Cluster of Excellence in Cellular Stress and Aging Associated Disease (CECAD), Cologne, Germany*

[10] *German Center for Neurodegenerative Diseases (DZNE), Bonn- Cologne, Germany*

[11] *Cognitive Neuroscience, Institute of Neuroscience and Medicine (INM-2), Research Center Jülich, Germany*

Correspondence to:
Kenan Steidel
University Hospital Marburg
Baldingerstraße
35034 Marburg
Department of Neurology
Email: steidel@staff.uni-marburg.de

Word count ~ 3890

Keywords:
Freezing of Gait, multimodal Imaging, PET, Functional Connectivity, Molecular Connectivity

Relevant conflicts of interests/financial disclosures: All Authors reported no financial disclosures related to the study.

Funding: The study was funded by the German Research Foundation (KFO 219, EG350/1-1)

Abbreviations: BDI-II = Beck's depression inventory II; BP_d = FDOPA-binding potential, DMN = default mode network; DU = dopaminergic uptake; FDOPA-PET = 6-[18F]fluoro-L-Dopa-PET; FOG-Q = freezing-of-gait questionnaire; FOG = freezing of gait; MC = Molecular connectivity, MMSE = Mini Mental Status Examination; NMS = non-motor symptom scale; PDQ-39 = Parkinson's disease questionnaire, PGS = postural instability and gait score; ROI = region of interest; rs-fMRI = resting state functional magnetic resonance tomography; UPDRS-III = Unified Parkinson's disease Rating Scale part III; VTA = ventral tegmental area

ABSTRACT

Freezing of gait is a common phenomenon of advanced Parkinson's disease. Besides locomotor function per se, a role of cognitive deficits has been suggested. Limited evidence of associated dopaminergic deficits points to caudatal denervation. Further, altered functional connectivity within resting-state networks with importance for cognitive functions has been described in freezers. A potential pathophysiological link between both imaging findings has not yet been addressed. The current study sought to investigate the association between dopaminergic pathway dysintegrity and functional dysconnectivity in relation to FOG severity and cognitive performance in a well-characterized PD cohort undergoing high-resolution 6-[18F]fluoro-L-DopaPET and functional MRI. The freezing of gait questionnaire was applied to categorize patients (n= 59) into freezers and non-freezers. A voxel-wise group comparison of 6-[18F]fluoro-L-Dopa PET with focus on striatum was performed between both well-matched and neuropsychologically characterized patient groups. Seed-to-voxel resting-state functional connectivity maps of the resulting dopamine depleted structures and dopaminergic midbrain regions were created and compared between both groups. For a direct between-group comparison of dopaminergic pathway integrity, a molecular connectivity approach was conducted on 6-[18F]fluoro-L-Dopa scans. With respect to striatal regions, freezers showed significant dopaminergic deficits in the left caudate nucleus, which exhibited altered functional connectivity with regions of the visual network. Regarding midbrain structures, the bilateral ventral tegmental area showed altered functional coupling to regions of the default mode network. An explorative examination of the integrity of dopaminergic pathways by molecular connectivity analysis revealed freezing-associated impairments in mesolimbic and mesocortical pathways. This study represents the first characterization of a link between dopaminergic pathway dysintegrity and altered functional connectivity in Parkinson's disease with freezing of gait and hints at a specific involvement of striatocortical and mesocorticolimbic pathways in freezers.

1. INTRODUCTION

Freezing of gait (FOG) is a common phenomenon of advanced Parkinson's disease (PD) and has been shown to severely affect patients' quality of life[1]. It comprises a transient disturbance in initiation or maintenance of steps, which is typically provoked by passing narrow spaces or turning[2]. Another provoking factor is dual tasking with cognitive effort[3], which underlines that cognitive function is mandatory for successful execution of gait and mobility[4,5]. Consequently, FOG patients perform significantly worse on cognitive tasks involving visuospatial skills[6–9], frontal executive functions[10–14] and attention[15–18]. An epidemiological and clinical description of FOG in a large cohort was published by Giladi and colleagues[19]. Analyses of the DATATOP-cohort revealed that around 27% of PD patients already experience FOG in early disease stages, indicating a distinct PD phenotype that favors freezing episodes[20].

Neuroimaging studies have thoroughly examined neurobiological correlates of FOG, including investigations using [^{18}F]fluorodeoxyglucose PET[21–28], perfusion studies using single-photon emission computed tomography (SPECT)[29–31], as well as various magnetic resonance imaging (MRI) modalities[18,32–35]. A growing body of studies performing connectivity analyses using diffusion tensor imaging or resting-state functional MRI (rs-fMRI)[36–42] suggests the involvement of tracts and brain regions engaged in frontal executive, visuospatial, limbic and locomotor performance with an emphasis on the right hemisphere[40,43] (see Song et al.[44] for review). Additionally, structural MRI studies reported volume loss in respective cortical areas[33,45–50].

Neuroimaging findings have contributed substantially to different models proposing mechanistic explanations for the episodic character of FOG[51]. Two of these models are not restricted to motor circuits and include one or more cognitive dimensions: 1.) the interference model assumes, that a network overload during conflicting motor, emotional and cognitive input processing[43] combined with maladaptive neural compensation causes freezing, 2.) the cognitive model proposes a response conflict facilitated by executive dysfunction as an underlying mechanism of FOG[51], which is supported by evidence of reduced functional connectivity of frontal areas in patients with FOG[52].

Fewer studies have concentrated on dopaminergic imaging in freezers[24,53], but limited evidence suggests stronger dopaminergic denervation of the caudate nucleus in patients with FOG[24]. This finding has been put into context with frontostriatal dysfunction in freezers[43], consistent with the cognitive model of FOG pathophysiology[12,51] and supported by alterations in resting-state networks with importance for cognitive processing observed by fMRI-studies, namely the default mode network (DMN) and frontoparietal network[37,52]. However, none of the studies has examined the direct association between dopaminergic pathways and resting-state functional connectivity in a cohort of PD patients with FOG to date.

Aside from structural and functional connectivity analyses, metabolic connectivity analyses have been attempted using molecular information obtained from [^{18}F]fluorodeoxyglucose-PET, which represents a more direct measure of neural activity. In this context, brain regions that are metabolically connected have been shown to display similar variances in radiotracer uptake[54]. The application of interregional correlation analyses[55] on a neurotransmitter level led to the emergence of molecular connectivity (MC) as a tool to visualize neurotransmitter pathways that coincide with anatomical pathways. With PET imaging using neurotransmitter-specific radioligands, serotonergic pathway dysintegrity could be displayed in patients with major depressive disorder[56]. Recently, this approach has been applied to 6-[^{18}F]fluoro-L-Dopa PET (FDOPA) to assess dopaminergic pathways of the midbrain[57,58] and its potential usefulness as a means of demonstrating dopaminergic dysintegrity also of extranigral pathways originating from the Ventral tegmental area (VTA) in diseases of the dopaminergic system has been postulated.

Despite a growing body of neuroimaging studies, the reported alterations within the above-stated networks in FOG patients have been inconsistent and multimodal studies are required to resolve interdependencies[43,44]. Furthermore, investigations of changes in dopaminergic signaling have been scarce. Here, we combined FDOPA-PET and rs-fMRI to multimodally characterize neurobiological mechanisms underlying FOG in a well-matched and neuropsychologically characterized subset of freezers (FOG+) and non-freezers (FOG-), focusing on dopaminergic pathways. Further, we analyzed the association between dopaminergic dysfunction and alterations in functional connectivity and their relation to FOG severity and behavioral variables. Finally, this is the first study that uses midbrain MC as a more direct correlate of dopaminergic pathway integrity to exploratively investigate the involvement of specific dopaminergic loops in PD patients with FOG.

In view of previous neuroimaging studies, we hypothesized that in freezers, dopaminergic denervation is specifically pronounced in the caudate and associated with altered striatocortical functional connectivity. Given the reported cognitive abnormalities, we further expected an involvement of the mesocorticolimbic pathways and associated dysregulations in resting-state networks involving the frontal cortex.

2. MATERIAL AND METHODS

2.1 Participants and clinical assessment

Within the KFO 219 cohort framework, 63 patients with idiopathic PD were recruited at the University Hospital of Cologne. Diagnosis was made according to UK-Brain-Bank criteria[59] by a movement disorder specialist. In accordance with the Declaration of Helsinki, ethical approval

was received from the local medical ethics committee (EK12-265) and informed consent was declared by each participant. PET imaging has been permitted by the Federal Bureau of Radiation. The study protocol, encompassing in- and exclusion criteria, cohort specification, non-motor symptoms and behavioral data, has been detailed in previous publications[60,61]. Motor severity was evaluated via the Unified PD rating scale (UPDRS) part III in the OFF-state[6263,64]. A postural and gait subscore (PGS) was calculated from UPDRS-III items 27-30. Left/right disease lateralization was calculated according to UPDRS-III subitems 20-26. Fifty-nine patients of the cohort completed the Freezing of gait questionnaire (FOG-Q)[65] and completed rs-fMRI acquisition; 44 patients of this cohort additionally underwent FDOPA-PET. FOG-severity was determined by FOG-Q total score; FOG status by item 3. Cognitive performance was tested using a neuropsychological test battery that included two tests per each of the five cognitive domains (attention, memory, language, executive and visuospatial) as detailed in Ruppert et al.[66]. As additional measures of global cognitive performance, the Mini-Mental State Examination (MMSE)[67] and the Parkinson's Neuropsychometric Dementia Assessment (PANDA)[68] were applied. Depressed mood was assessed with Beck's Depression Inventory II (BDI-II) [69]and quality of life with the Parkinson's Disease Questionnaire 39 (PDQ39)[70].

2.2 Neuroimaging Data Acquisition and (Pre-)processing

2.2.1 FDOPA-PET

PET scans were performed in dopaminergic OFF-state after overnight fasting in a high-resolution research tomograph (ECAT, HRRT, Siemens, Erlangen, Germany) at the Max-Planck-Institute for Metabolism Research, Cologne. The detailed acquisition protocol was described in previous publications[60,61]. Resulting frames were motion-corrected via rigid-body transformation and the average of frames number four to nine was used for further analysis. Stereotactic normalization was performed by non-linear registration to an established FDOPA-PET template in Montreal Neurological Institute (MNI)[71] space. Images were spatially smoothed with a 3-dimensional Gaussian filter of 6 mm full width at half maximum (FWHM) using SPM12 (www.fil.ion.ucl.ac.uk/spm/software/spm12).

2.2.2 Intensity Normalization and Molecular Connectivity

The mean FDOPA uptake (DU) was extracted subject-wise from an occipital reference region with no relevant dopaminergic activity. Specific voxel-wise FDOPA-binding potential (BP_d) values were calculated via the following formula, which was initially established for ^{123}I-Ioflupane SPECT analysis[72], using the ImageCalculator tool in SPM:

$$BPd = \frac{\mathrm{DU(voxel)} - \mathrm{DU(occipital)}}{\mathrm{DU(occipital)}}$$

DU from an occipital reference region from the automated anatomical labeling atlas 3 (AAL 3)[73] obtained via wfu_PickAtlas (https://www.nitrc.org/projects/wfu_pickatlas/) was extracted from spatially normalized images via MarsBaR software (http://marsbar. sourceforge.net). Group comparisons between FOG+ and FOG- subsamples were performed by applying voxel-wise two-sample *t*-tests with small volume correction (SVC) for striatum (AALv3) in SPM12 using a threshold of $p<0.05$ with cluster level family-wise error (FWE) correction for multiple comparisons. Resulting clusters were exported, binarized, used for functional connectivity analyses, and to compare ROI-wise BP_d between differently lateralized patients. For a schematic overview of the applied workflow see figure 1.

MC investigations to analyze mesocorticolimbic dopaminergic pathways were implemented by ROI-wise interregional correlation analysis. BP_d was extracted separately for each region of the mesocortical or mesolimbic dopamine system on a single subject level (regions from AALv3, see supplements) using MarsBaR. ROI-based correlations (Spearman's ρ) with the bilateral VTA were calculated across subjects and subsequently compared between freezers and non-freezers via Fisher's z-test using R[74] with correction for multiple comparisons using false-discovery-rate (FDR) (for a schematic overview see figure 1). The same procedure was applied to the bilateral substantia nigra as a seed volume for nigrostriatal pathways. The corresponding atlas regions are listed in supplementary table 2.

2.2.3 Resting-state fMRI

FMRI and T1-weighted images were acquired on a 3T Siemens Magnetom Prisma using the software system syngo MR D13D with the acquisition parameters as detailed elsewhere. Technical details of fMRI images were as follows: repetition time, 776 ms, echo time, 37.4 ms, 617 time points, 72 slices: voxel size, 2x2x2 mm. Preprocessing was carried out using the SPM toolbox CONN v17[75] following the default pipeline as detailed in previous publications[60].

2.2.4 Rs-fMRI Connectivity Analyses

Functional connectivity investigations were performed by applying seed-based correlation analyses using Conn. In order to analyze the connectivity profile of regions with differences in dopaminergic activity between FOG+ and FOG- patients, we used the cluster obtained by between-group comparison in the PET modality as seed volume for seed-based correlation analysis. To examine the influence of the mesocorticolimbic dopamine system on resting-state networks, additional analyses were performed with the bilateral VTA atlas ROI (AALv3) as seed. Connectivity maps obtained at group-level were compared by applying the contrasts FOG+>FOG-

or FOG+<FOG-, thresholded at p<0.05 cluster level FWE-corrected for multiple testing. Functional connectivity values were exported for significant clusters and entered in correlation analyses with clinical data via Spearman's ρ or Pearsons' r, observing normality assumptions. Results were considered significant if $p < 0.05$ after applying the false-discovery rate (FDR) correction for multiple comparisons. Likewise, we investigated the direct impact of dopaminergic degeneration in seed ROIs on the respective functional connectivity by applying correlation analysis.

2.3 Clinical and Behavioral Data

Statistical analyses of demographic, clinical and behavioral variables in FOG+ and FOG- subsamples were conducted in R[74]. After testing for normal distributions via Shapiro-Wilk-test, group comparisons were performed using Welch's *t*-test or Mann-Whitney U-test and correlations via Spearman's ρ or Pearson's r as appropriate. Chi-squared test was applied for comparisons of dichotomous variables. Differences in cognitive z-scores were examined using an analysis of covariance (ANCOVA) with BDI-II as covariate as previously suggested[76].

3. RESULTS

3.1 Demographic, Clinical and Behavioral Data

There was no significant difference in age, sex, disease duration and UPDRS-III between FOG groups, and group sizes were quite similar (see Table 1). Significantly higher FOG-severity (p<0.001) and PGS (p=0.009) were observed in freezers compared to non-freezers, but no significant difference in UPDPRS-III scores (p=0.135) or lateralization of motor impairment (p=0.130). Moreover, we observed significantly higher BDI-II scores (p=0.018) and higher Parkinson's disease questionnaire (PDQ-39) scores (p=0.012) in FOG+ patients, indicating a higher level of depressed mood and reduced quality of life in FOG+ patients. Additionally, there were no significant group differences in Hoehn & Yahr stages, levodopa equivalent daily doses, and levodopa response. Further, there was no significant correlation between levodopa response and FOG-Q scores. We found no group differences in z-values of domain-specific z-scores or the cognitive composite z-scores (Table 1) and also not in MMSE or PANDA scores. These differences became significant after including BDI-II as covariate in the case of visuo-spatial z-score (ANCOVA, F=5.36, p=0.024) with a worse performance in FOG- patients and remained non-significant for global cognition z-score (F=2.56, p=0.12). In the cohort of patients who received FDOPA-PET, there were no significant differences in BDI-II and PDQ-39 scores, but significantly lower visuo-spatial z-scores (p=0.032) and global cognition z-scores (p=0.026, see supplements).

Table 1: Demographic and Clinical Data

	FOG+ n = 27	FOG- n = 32	p-value	Test statistic
Age [years]	66.5 ± 8.5	64.4 ± 10.4	0.397	t=0.85
Sex m/f	17/10	23/9	0.465	X^2=0.53
Laterality (right/left/equal)	8/18/1	16/13/3	0.130	X^2=4.08
Disease duration [years]	5.4 ± 3.8	4.6 ± 3.3	0.444	W=482.5
FOG-severity	10.2 ± 4.5	2.0 ± 1.6	<0.001	W=858.0
UPDRS-III	27.2 ± 10.3	22.4 ± 7.8	0.135	W=530.5
PGS	2.8 ± 2.2	1.34 ± 1.43	0.009	W=601.5
BDI-II	11.9 ± 8.1	8.0 ± 6.7	0.018	W=587.0
PDQ39	26.44 ± 15.7	18.7 ± 17.3	0.012	W=598.0
Hoehn & Yahr	2.4 ± 0.5	2.2 ± 0.4	0.185	W=511.0
LEDD [mg]	517.8 ± 302.7	458.1 ± 294.0	0.330	W=496.5
Levodopa response	0.27 ± 0.1	0.29 ± 0.1	0.599	t=-0.53
Neuropsychological Data				
MMST	28.7 ± 1.3	28.2 ± 2.0	0.352	W=411.0
PANDA	23.5 ± 4.2	23.4 ± 5.3	0.580	W=516.5
Executive z-score	-0.2 ± 0.7	-0.2 ± 0.6	0.839	W=402.5
Memory z-score	-0.3 ± 1.1	-0.3 ± 1.1	0.976	W=429.5
Attention z-score	-0.1 ± 0.7	-0.2 ± 0.9	0.749	W=-453.5
Language z-score	-0.2 ± 0.8	0.1 ± 0.6	0.434	W=466.5
Visuo-spatial z-score	-0.1 ± 0.8	-0.6 ± 1.2	0.079	W=545.5
Global cognition z-score	-0.1 ± 0.4	-0.2 ± 0.5	0.268	t=1.12

Numeric variables are shown as mean ± standard deviation. Group comparisons were calculated using Welch's t-test or Wilcoxon-test. Nominal variables were compared by Chi-squared test. Levodopa response is defined as ratio of UPDRS-III in OFF and ON state. Abbreviations: LEDD: Levodopa equivalent daily dose, PDQ39: Parkinson's Disease Questionnaire 39, PANDA: Parkinson's Neuropsychometric Dementia Assessment, MMST: Mini-Mental Status Examination, UPDRS-III: Unified Parkinson's Disease Rating Scale, PGS: Postural-Gait-Score

3.2 Neuroimaging

Voxel-wise between-group analysis of FDOPA-PET scans revealed significantly reduced BP_d values in the left caudate nucleus in FOG+ patients compared to FOG- patients (p_{FWE}= 0.008, Fig. 2A top). When patient groups were further subdivided into left- and right-dominant PD, BP_d values of the caudate cluster were significantly lower in the FOG+ group regardless of symptom laterality (left: t=-2.54, p=0.022; right: t=-2.90, p=0.011). A within-group comparison in patients with FOG+ revealed no significant difference in BP_d uptake of the left caudate between the left- and right-lateralized patients (t=-0.64, p=0.540).

To further evaluate the integrity of mesocorticolimbic pathways in both patient groups, we conducted a explorative MC analysis. It revealed lower correlations of BP_d in regions of the mesolimbic pathway between the bilateral VTA and the bilateral anterior cingulate cortex (left: p= 0.015, right: p=0.010), the right parahippocampal gyrus (p=0.010), and the right amygdala (p=0.010) in FOG+ compared to FOG- patients. Moreover, we observed reduced covariance with the right ventromedial prefrontal cortex (p=0.026) corresponding to the mesocortical dopamine system (see Fig. 3). Using the bilateral substantia nigra as a seed, we found no significant difference in MC corresponding to the nigrostriatal dopamine system.

The seed-based correlation analysis revealed increased functional connectivity between the dopamine deficient left caudate cluster and the right visual cortex in FOG+ patients compared to FOG- patients (p_{FWE}<0.05, Fig. 4A, Table 2). In addition, we performed this correlation analysis with atlas-derived regions of dopaminergic nuclei (VTA AALv3) to analyze functional connectivity of the mesocorticolimbic and nigrostriatal pathways in both groups. We found increased functional connectivity between the bilateral VTA and key structures of the DMN, such as right superior frontal gyrus as well as bilateral angular gyrus, bilateral superior lateral occipital cortex and bilateral precuneus in FOG+ patients compared to FOG- patients (p_{FWE}<0.05, Fig. 4B, Table 2), whereas no altered connectivity could be found for substantia nigra. Regarding correlations with dopaminergic degeneration, we found a significant negative correlation between BP_d of the left caudate and its functional connectivity to the right visual cortex (r=-0.540, p<0.001).

Correlation analyses between neuroimaging findings and clinical parameters revealed significant positive correlations between FOG-Q-scores and BP_d of the left caudate (r=-0.49, p=0.016) and between functional connectivity values of the bilateral VTA and the right superior frontal gyrus (r=0.56, p<0.001), left superior lateral occipital cortex (r =0.54, p<0.001), right superior lateral occipital cortex (r=0.55, p<0.001) in the total PD sample. Besides, PGS and FOG-Q-score were significantly related (r= 0.51 p<0.001). However, no significant correlations with FOG severity were observed in the FOG+ subsample. For evaluation of a potential impact of cognitive impairment on FOG, we performed correlation analyses between cognition z-scores and FOG-Q

scores, which yielded significant negative correlations in the FOG+ subsample for global cognition z-score (r=-0.41 p=0.025). In the subset of patients, who only received FDOPA-PET, FOG severity was also negatively correlated with performance in cognitive tests (r=-0.55, p=0.010 for executive z-score; r=-0.62, p=0.003 for global cognition z-score; r=-0.52, p=0.016 for PANDA).

Table 2: Results of Neuroimaging Analysis

Modality	Region	MNI Coordinates	Statistic		Cluster Size
		x/y/z	T-value	p-value (FWE)	
FDOPA-PET t-test (FOG+<FOG-)	CAU_L	-8/8/10	3.84	0.008	112
rs-fMRI CAUL (FOG+>FOG-)	CAL_R Occi_Sup_R	20/-88/4	5.38	0.033	70
rs-fMRI VTAbil (FOG+>FOG-)	Parietal_inf_L Occi_Mid_L AG_L	-36/-74/40	5.71	< 0.001	447
	AG_R Occi_Mid_R	48/-72/36	4.91	< 0.001	237
	SFG_R	22/30/46	5.21	< 0.001	134
	PCUN_L CAL_L	-14/-58/16	4.84	0.014	74
	PCUN_R CAL_R	16/-44/4	4.69	0.012	76

Neuroimaging results by modality and contrast. T-values were calculated using SPM12. Rs-fMRI analyses were conducted in Conn. The bilateral VTA (AALv3) was used as seed region for FDOPA-PET MC. Seed regions for seed-based correlation analysis were CAU_L and bilateral VTA (VTAbil). Abbreviations: AG_L: angular gyrus left, AG_R: angular gyrus right, CAL: calcarine sulcus, CAU_L: left caudate nucleus, Occi_Mid_L: mid occipital cortex left, Occi_Mid_R: mid occipital cortex right, Occi_Sup_R: superior occipital cortex right, Parietal_Inf_L: inferior parietal cortex left, PCUN: precuneus, SFG_R: right superior frontal gyrus.

4. DISCUSSION

The current study provides evidence for a more pronounced dopaminergic deficit confined to the caudate nucleus in the OFF-state in FOG+ patients. The dopamine-deficient caudate and atlas-based midbrain regions also showed changes in functional connectivity to the visual cortex and regions of the DMN in freezers compared to non-freezers. Moreover, we conducted a FDOPA-PET molecular connectivity approach to assess the integrity of midbrain dopaminergic pathways. This approach hinted at an impairment of dopaminergic midbrain pathways projecting to the cingulate and ventromedial cortex, revealing evidence for a potential involvement of mesolimbic and mesocortical pathways in FOG-associated functional dysconnectivity.

4.1 Caudatal Dopamine Depletion and the Visual Cortex in FOG

Past dopaminergic imaging studies were able to assign FOG-associated striatal dopaminergic hypometabolism[23,53] mainly to the right caudate[24]. In the current study, we compared groups not differing in disease duration, whereas most previous studies were confounded by longer disease duration in freezers[23,24]. In contrast, FOG+ patients in our cohort exhibited a stronger dopaminergic deficit in the left caudate, which was true for both left- and right- lateralized individuals. As there were no differences between left- and right-lateralized freezers in this respect, the finding of a more dopamine-depleted left caudate in our cohort can be interpreted as FOG-related. Additionally, we could ascertain the interrelation between this imaging finding and FOG-Q in the overall cohort. A crucial role of the caudate and its striatocortical loops in FOG has been suggested previously [43] and caudatal volume has been shown to be related to gait control in older subjects in structural MRI studies[77].

Besides reduced BP_d in the left caudate, we found increased functional connectivity of the dopamine depleted cluster to a part of the visual resting-state network. Previous studies reported reduced dopamine transporter levels in the caudate in response to a walking exercise in PD patients and inferred that it is a key driver of parkinsonian gait, specifically sustained gait performance cued by primarily visual external stimuli[78]. Further, impaired functional connectivity[52], reduced glucose metabolism[23], or increased BOLD responses[13] of primary and secondary visual areas as well as an involvement of visuospatial pathways[6] has been reported in freezers. Our findings are suggestive of a stronger coupling between the caudate and the visual cortex in FOG secondarily to dopamine depletion, and hence do not only underpin previous findings but also reveal the first explanation for an association between imaging findings in both regions. Several studies revealed evidence for a visual corticostriatal loop involving the caudate in mammals and postulated a role in visuospatial functioning and visuomotor control. Functional and structural connections between the caudate and occipital areas have been described before[78,79]. However, since the visual loop was not the focus of these studies, the knowledge about

which visual region projects to which part of the striatum is still limited[81]. Evidence in humans largely resists on tractography based on diffusion imaging and points towards a convergence of posterior parietal, orbitofrontal, dorsolateral prefrontal projections in the mainly ipsilateral rostral caudate[79]. The inability to obtain histologically described contralateral corticostriatal projections may be due to the inherent limitation of diffusion-weighted imaging for tracking contralateral projections[79].

4.2 Dopaminergic DMN Modulation in FOG

While focusing on functional connectivity in resting-state networks by using independent component analysis approaches, previous rs-fMRI studies mainly found reduced functional connectivity in DMN regions, which correlated with FOG severity[52,37]. Using dopaminergic midbrain regions as seed volumes in a seed-based correlation analysis approach, we found increased functional connectivity between the bilateral VTA and DMN regions, including the superior frontal gyrus and bilateral lateral occipital gyri in FOG+ patients. Further, functional connectivity between the VTA and superior frontal and superior lateral occipital regions correlated significantly with FOG-Q in the entire study sample.

According to a novel definition, subcortical structures have been underestimated in DMN specifications so far[82]. Recently published work assigns the VTA a role as key subcortical structure of the DMN[82]. Comprehensive analyses on neurotransmitter signaling and its influence on resting-state networks further stated that monoaminergic signaling modulates functional coupling of cortical resting-state networks via subcortical-cortical loops[83]. In this context, dopamine antagonists have been reported to increase DMN connectivity[84] and dopaminergic signaling was found to decrease functional connectivity in the DMN in previous studies and suspected as an active suppression mechanism in situations with external demanding attention[83,85]. In FOG, the synchronized activity between dopaminergic midbrain regions and the DMN is remarkably altered according to our findings.

4.3 Dopaminergic Pathway Dysintegrity in FOG

To further investigate the impact of dopaminergic signaling on functional dysconnectivity, we applied ROI-wise MC[57] approach, which revealed lower covariance in BP_d of the bilateral VTA with parts of the right ventromedial prefrontal cortex as well as bilateral anterior cingulate cortex, right amygdala and parahippocampal gyrus suggesting an impairment of dopaminergic transmission in mesocortical and mesolimbic pathways in FOG+ compared to FOG- patients. In

contrast to the observed univariate deficit, we found no hints for nigrostriatal deficits using this method.

In accordance with our data, previous literature stated that reduced dopaminergic function in the orbitofrontal cortex as a part of the mesolimbic pathway contributes to gait disturbances in PD[78], and impaired activity of mesolimbic areas has been reported in freezers, especially in episodes of increased cognitive load[34]. Moreover, resulting clusters cover parts of the DMN as well, which corresponds well with the reported functional connectivity dysregulation between the VTA and DMN regions, providing further evidence for DMN dysregulation as a consequence of loss of mesocortical dopaminergic pathway integrity. Being strongly associated with frontal function[86], respectively motivation, and the translation into action[87], impairment of these regions fits well into the cognitive and response conflict model of FOG pathophysiology[12,51,88].

The present findings of reduced dopaminergic signaling and the concomitant alterations in functional connectivity on a network level, provide a possible explanation why FOG mostly responds to dopaminergic therapy[89]. Since all imaging procedures in the current study were performed in the OFF-state, neurobiological correlates exclusively represent dysregulations observed in freezers in the absence of dopaminergic medication. According to recently published articles, future investigations should consider clear distinctions between levodopa-responsive and nonresponsive FOG as well as levodopa-induced FOG, which have been postulated as separate clinical subtypes and suspected to represent distinct pathophysiological entities[90]. Although levodopa-responsive OFF freezing has been reported as the most common form[91], which is likely to predominate in the current cohort, further investigations should include consecutive imaging sessions and clinical examinations with levodopa challenges to provide detailed insights into pathophysiology of freezing subtypes. A more comprehensive view of different subtypes with multimodal imaging could ultimately promote optimized therapy and reduce concomitant events such as falls in freezers.

4.4 Limitations

The primary limitations comprise the classification of patients into freezers and non-freezers via a questionnaire and the associated uncertainty of a self-reporting system compared to clinical evaluation of freezing episodes. As FOG status is defined based on a single FOG-Q item, FOG-severity can only be considered as an adequate measure of this clinical phenomenon in FOG+ patients. High FOG-Q total-scores in FOG- patients may be confounded by comorbidities such as arthrosis. Nevertheless, FOG-Q-scores can be interpreted as a measure of gait impairment even in non-freezers, which is supported by a positive correlation of PGS and FOG-Q-score. Since all imaging procedures were performed in the OFF-state, the described results are likely to reflect

the phenomenon of OFF-freezing. The effect of levodopa was not formally addressed by levodopa challenge and measures of FOG in ON and OFF condition. An inference on levodopa-induced ON-freezing, possibly driven by additional impairments in glutamatergic and cholinergic systems[92], is therefore beyond the scope of this study. To further elucidate its pathophysiology, future studies should include separate analysis of freezing subtypes. The fact that no direct deficit in cognitive and visuospatial performance could be shown in the FOG+ group compared to the FOG- group could be related to the exclusion of advanced disease stages. Nevertheless, the direct relationship between FOG severity and both parameters shows that the individual expression of both global cognition and visuospatial abilities are contributing factors of freezing of gait. Due to using averaged FDOPA-PET scans rather than time-series, MC analyses can solely be conducted on a group level, preventing the possibility to obtain connectivity values on a single subject level in contrast to functional connectivity measurements in rs-fMRI. Finally, the data-driven and a priori defined seed selection applied in the current study prevented the identification of other networks that might also contribute to freezing. More comprehensive insights could be gained if other neurotransmitter systems are integrated into the imaging analysis, as the dopaminergic system may not be the only system involved[92,93].

5. CONCLUSION

In conclusion, our data provide evidence for reduced dopamine metabolism in the caudate nucleus and reduced covariance in mesolimbic and mesocortical pathways in PD patients with FOG. The impaired dopamine signaling in these regions apparently leads to a modulation of functional coupling via subcortical-cortical loops, thereby contributing to clinical gait disturbances. To the best of our knowledge this is the first study to multimodally assess dopaminergic pathways in FOG and analyze their influence on functional connectivity via combining FDOPA-PET and rs-fMRI. Furthermore, MC in the form of covariance of DU has first been applied to PD patients with FOG as a novel method to demonstrate dopaminergic pathway integrity. In essence, our data provide further inside in how the combination of different imaging techniques can help to understand the underlying mechanisms of freezing and its responsiveness to dopaminergic therapy.

6. REFERENCES

1. Moore O, Peretz C, Giladi N. Freezing of gait affects quality of life of peoples with Parkinson's disease beyond its relationships with mobility and gait. Mov Disord. 2007;22:2192–2195.

2. Nutt JG, Bloem BR, Giladi N, Hallett M, Horak FB, Nieuwboer A. Freezing of gait: Moving forward on a mysterious clinical phenomenon. Lancet Neurol. 2011. p. 734–744.

3. Spildooren J, Vercruysse S, Desloovere K, Vandenberghe W, Kerckhofs E, Nieuwboer A. Freezing of gait in Parkinson's disease: The impact of dual-tasking and turning. Mov Disord. 2010;25:2563–2570.

4. Peterson DS, King LA, Cohen RG, Horak FB. Cognitive contributions to freezing of gait in parkinson disease: Implications for physical rehabilitation. Phys Ther [online serial]. American Physical Therapy Association; 2016;96:659–670. Accessed at: /pmc/articles/PMC4858659/?report=abstract. Accessed August 18, 2020.

5. Giladi N, Hausdorff JM. The role of mental function in the pathogenesis of freezing of gait in Parkinson's disease. J Neurol Sci. 2006;248:173–176.

6. Lord S, Archibald N, Mosimann U, Burn D, Rochester L. Dorsal rather than ventral visual pathways discriminate freezing status in Parkinson's disease. Park Relat Disord [online serial]. Parkinsonism Relat Disord; 2012;18:1094–1096. Accessed at: https://pubmed.ncbi.nlm.nih.gov/22705127/. Accessed August 18, 2020.

7. Almeida QJ, Lebold CA. Freezing of gait in Parkinson's disease: A perceptual cause for a motor impairment? J Neurol Neurosurg Psychiatry [online serial]. BMJ Publishing Group; 2010;81:513–518. Accessed at: https://pubmed.ncbi.nlm.nih.gov/19758982/. Accessed August 18, 2020.

8. Cowie D, Limousin P, Peters A, Day BL. Insights into the neural control of locomotion from walking through doorways in Parkinson's disease. Neuropsychologia [online serial]. Neuropsychologia; 2010;48:2750–2757. Accessed at: https://pubmed.ncbi.nlm.nih.gov/20519135/. Accessed August 18, 2020.

9. Nantel J, McDonald JC, Tan S, Bronte-Stewart H. Deficits in visuospatial processing contribute to quantitative measures of freezing of gait in Parkinson's disease. Neuroscience [online serial]. Neuroscience; 2012;221:151–156. Accessed at: https://pubmed.ncbi.nlm.nih.gov/22796080/. Accessed August 18, 2020.

10. Amboni M, Cozzolino A, Longo K, Picillo M, Barone P. Freezing of gait and executive functions in patients with Parkinson's disease. Mov Disord [online serial]. Mov Disord; 2008;23:395–400. Accessed at: https://pubmed.ncbi.nlm.nih.gov/18067193/. Accessed August 18, 2020.

11. Vandenbossche J, Deroost N, Soetens E, et al. Freezing of gait in Parkinson disease is associated with impaired conflict resolution. Neurorehabil Neural Repair [online serial]. Neurorehabil Neural Repair; 2011;25:765–773. Accessed at: https://pubmed.ncbi.nlm.nih.gov/21478498/. Accessed August 18, 2020.

12. Vandenbossche J, Deroost N, Soetens E, et al. Conflict and freezing of gait in Parkinson's disease: Support for a response control deficit. Neuroscience [online serial]. Neuroscience; 2012;206:144–154. Accessed at: https://pubmed.ncbi.nlm.nih.gov/22265727/. Accessed August 18, 2020.

13. Matar E, Shine JM, Naismith SL, Lewis SJG. Using virtual reality to explore the role of conflict resolution and environmental salience in Freezing of Gait in Parkinson's disease. Park Relat Disord [online serial]. Parkinsonism Relat Disord; 2013;19:937–942. Accessed at: https://pubmed.ncbi.nlm.nih.gov/23831480/. Accessed August 18, 2020.

14. Cohen RG, Klein KA, Nomura M, et al. Inhibition, executive function, and freezing of gait. J Parkinsons Dis [online serial]. I O S Press; 2014;4:111–122. Accessed at: https://pubmed.ncbi.nlm.nih.gov/24496099/. Accessed August 18, 2020.

15. Hall JM, Shine JM, Walton CC, et al. Early phenotypic differences between Parkinson's disease patients with and without freezing of gait. Park Relat Disord [online serial]. Elsevier BV; 2014;20:604–607. Accessed at: https://pubmed.ncbi.nlm.nih.gov/24679901/. Accessed August 18, 2020.

16. Naismith SL, Shine JM, Lewis SJG. The specific contributions of set-shifting to freezing of gait in Parkinson's disease. Mov Disord [online serial]. John Wiley and Sons Inc.; 2010;25:1000–1004. Accessed at: https://pubmed.ncbi.nlm.nih.gov/20198644/. Accessed August 18, 2020.

17. Peterson DS, Fling BW, Mancini M, Cohen RG, Nutt JG, Horak FB. Dual-task interference and brain structural connectivity in people with Parkinson's disease who freeze. J Neurol Neurosurg Psychiatry [online serial]. BMJ Publishing Group; 2015;86:786–792. Accessed at: https://pubmed.ncbi.nlm.nih.gov/25224677/. Accessed August 18, 2020.

18. Shine JM, Naismith SL, Palavra NC, et al. Attentional set-shifting deficits correlate with the severity of freezing of gait in Parkinson's disease. Park. Relat. Disord. 2013. p. 388–390.

19. Giladi N, McMahon D, Przedborski S, et al. Motor blocks in Parkinson's disease. Neurology. 1992;42:333–339.

20. Giladi N, McDermott MP, Fahn S, et al. Freezing of gait in PD: Prospective assessment in the DATATOP cohort. Neurology. 2001;56:1712–1721.

21. Park HK, Kim JS, Im KC, et al. Functional brain imaging in pure Akinesia with Gait freezing: [18F] FDG PET and [18F] FP-CIT PET analyses. Mov Disord [online serial]. Mov Disord; 2009;24:237–245. Accessed at: https://pubmed.ncbi.nlm.nih.gov/18951539/. Accessed August 19, 2020.

22. Gallardo MJ, Cabello JP, Corrales MJ, et al. Freezing of gait in Parkinson's disease: functional neuroimaging studies of the frontal lobe [online]. Neurol. Res. Taylor and Francis Ltd.; 2018. p. 900–905. Accessed at: https://pubmed.ncbi.nlm.nih.gov/29985119/. Accessed August 19, 2020.

23. Zhou Y, Zhao J, Hou Y, Su Y, Chan P, Wang Y. Dopaminergic pathway and primary visual cortex are involved in the freezing of gait in parkinson's disease: A PET-CT study. Neuropsychiatr Dis Treat [online serial]. Dove Medical Press Ltd.; 2019;15:1905–1914. Accessed at: https://pubmed.ncbi.nlm.nih.gov/31410003/. Accessed August 19, 2020.

24. Bartels AL, de Jong BM, Giladi N, et al. Striatal dopa and glucose metabolism in PD patients with freezing of gait. Mov Disord. 2006;21:1326–1332.

25. del Olmo MF, Arias P, Furio MC, Pozo MA, Cudeiro J. Evaluation of the effect of training using auditory stimulation on rhythmic movement in Parkinsonian patients-a combined motor and [18F]-FDG PET study. Park Relat Disord. 2006;12:155–164.

26. Chul HL, Aalto S, Rinne JO, et al. Different cerebral cortical areas influence the effect of subthalamic nucleus stimulation on Parkinsonian motor deficits and freezing of gait. Mov Disord [online serial]. Mov Disord; 2007;22:2176–2182. Accessed at: https://pubmed.ncbi.nlm.nih.gov/17712844/. Accessed August 19, 2020.

27. Tard C, Delval A, Devos D, et al. Brain metabolic abnormalities during gait with freezing in Parkinson's disease. Neuroscience [online serial]. Elsevier Ltd; 2015;307:281–301. Accessed at: https://pubmed.ncbi.nlm.nih.gov/26341909/. Accessed August 19, 2020.

28. Mitchell T, Potvin-Desrochers A, Lafontaine AL, Monchi O, Thiel A, Paquette C. Cerebral metabolic changes related to freezing of gait in Parkinson disease. J Nucl Med [online serial]. Society of Nuclear Medicine Inc.; 2019;60:671–676. Accessed at: https://pubmed.ncbi.nlm.nih.gov/30315142/. Accessed August 19, 2020.

29. Fabre N, Brefel C, Sabatini U, et al. Normal frontal perfusion in patients with frozen gait. Mov Disord [online serial]. 1998;13:677–683. Accessed at: http://doi.wiley.com/10.1002/mds.870130412. Accessed January 16, 2020.

30. Matsui H, Ukada F, Miyoshi T, et al. Three-dimensional stereotactic surface projection study of freezing of gait and brain perfusion image in Parkinson's disease. Mov Disord. 2005;20:1272–1277.

31. Mito Y, Yoshida K, Yabe I, et al. Brain SPECT analysis by 3D-SSP and clinical features of Parkinson's disease. Hokkaido Igaku Zasshi. 2006;81:15–23.

32. Shine JM, Ward PB, Naismith SL, Pearson M, Lewis SJG. Utilising functional MRI (fMRI) to explore the freezing phenomenon in Parkinson's disease. J Clin Neurosci. Churchill Livingstone; 2011;18:807–810.

33. Snijders AH, Leunissen I, Bakker M, et al. Gait-related cerebral alterations in patients with Parkinson's disease with freezing of gait. Brain. 2011;134:59–72.

34. Shine JM, Matar E, Ward PB, et al. Differential Neural Activation Patterns in Patients with Parkinson's Disease and Freezing of Gait in Response to Concurrent Cognitive and Motor Load. PLoS One. 2013;8.

35. Shine JM, Matar E, Ward PB, et al. Exploring the cortical and subcortical functional magnetic resonance imaging changes associated with freezing in Parkinson's disease. Brain. Oxford University Press; 2013;136:1204–1215.

36. Fling BW, Cohen RG, Mancini M, et al. Functional reorganization of the locomotor network in parkinson patients with freezing of gait. PLoS One. 2014;9.

37. Canu E, Agosta F, Sarasso E, et al. Brain structural and functional connectivity in Parkinson's disease with freezing of gait. Hum Brain Mapp [online serial]. John Wiley and Sons Inc.; 2015;36:5064–5078. Accessed at: https://pubmed.ncbi.nlm.nih.gov/26359798/. Accessed August 19, 2020.

38. Lenka A, Naduthota RM, Jha M, et al. Freezing of gait in Parkinson's disease is associated with altered functional brain connectivity. Park Relat Disord [online serial]. Elsevier Ltd; 2016;24:100–106. Accessed at: https://pubmed.ncbi.nlm.nih.gov/26776567/. Accessed August 19, 2020.

39. Vervoort G, Heremans E, Bengevoord A, et al. Dual-task-related neural connectivity changes in patients with Parkinson' disease. Neuroscience [online serial]. Elsevier Ltd; 2016;317:36–46. Accessed at: https://pubmed.ncbi.nlm.nih.gov/26762801/. Accessed August 19, 2020.

40. Bharti K, Suppa A, Tommasin S, et al. Neuroimaging advances in Parkinson's disease with freezing of gait: A systematic review. NeuroImage Clin. Elsevier Inc.; 2019. p. 102059.

41. Gilat M, Ehgoetz Martens KA, Miranda-Domínguez O, et al. Dysfunctional Limbic Circuitry Underlying Freezing of Gait in Parkinson's Disease. Neuroscience [online serial]. Elsevier Ltd; 2018;374:119–132. Accessed at: https://pubmed.ncbi.nlm.nih.gov/29408498/. Accessed August 19, 2020.

42. Maidan I, Jacob Y, Giladi N, Hausdorff JM, Mirelman A. Altered organization of the dorsal attention network is associated with freezing of gait in Parkinson's disease. Park Relat Disord [online serial]. Elsevier Ltd; 2019;63:77–82. Accessed at: https://pubmed.ncbi.nlm.nih.gov/30827838/. Accessed August 19, 2020.

43. Fasano A, Herman T, Tessitore A, Strafella AP, Bohnen NI. Neuroimaging of freezing of gait. J Parkinsons Dis [online serial]. IOS Press; 2015;5:241–254. Accessed at: https://pubmed.ncbi.nlm.nih.gov/25757831/. Accessed August 19, 2020.

44. Song W, Raza HK, Lu L, et al. Functional MRI in Parkinson's disease with freezing of gait: a systematic review of the literature. Neurol Sci. 2021;42:1759–1771.

45. Kostić VS, Agosta F, Pievani M, et al. Pattern of brain tissue loss associated with freezing of gait in Parkinson disease. Neurology. Lippincott Williams and Wilkins; 2012;78:409–416.

46. Rosenberg-Katz K, Herman T, Jacob Y, Giladi N, Hendler T, Hausdorff JM. Gray matter atrophy distinguishes between Parkinson disease motor subtypes. Neurology. 2013;80:1476–1484.

47. Herman T, Rosenberg-Katz K, Jacob Y, Giladi N, Hausdorff JM. Gray matter atrophy and freezing of gait in Parkinson's disease: Is the evidence black-on-white? Mov Disord. 2014;29:134–139.

48. Herman T, Giladi N, Hausdorff JM. Neuroimaging as a window into gait disturbances and freezing of gait in patients with Parkinson's disease. Curr Neurol Neurosci Rep. 2013;13.

49. Pietracupa S, Suppa A, Upadhyay N, et al. Freezing of gait in Parkinson's disease: gray and white matter abnormalities. J Neurol [online serial]. Dr. Dietrich Steinkopff Verlag GmbH and Co. KG; 2018;265:52–62. Accessed at: https://pubmed.ncbi.nlm.nih.gov/29128929/. Accessed August 19, 2020.

50. Vastik M, Hok P, Valosek J, Hlustik P, Mensikova K, Kanovsky P. Freezing of gait is associated with cortical thinning in mesial frontal cortex. Biomed Pap [online serial]. PALACKY UNIV; 2017;161:389–396. Accessed at: https://pubmed.ncbi.nlm.nih.gov/28928491/. Accessed August 19, 2020.

51. Nieuwboer A, Giladi N. Characterizing freezing of gait in Parkinson's disease: Models of an episodic phenomenon [online]. Mov. Disord. Mov Disord; 2013. p. 1509–1519. Accessed at: https://pubmed.ncbi.nlm.nih.gov/24132839/. Accessed September 17, 2020.

52. Tessitore A, Amboni M, Esposito F, et al. Resting-state brain connectivity in patients with Parkinson's disease and freezing of gait. Park Relat Disord. 2012;18:781–787.

53. Bohnen NI, Frey KA, Studenski S, et al. Extra-nigral pathological conditions are common in Parkinson's disease with freezing of gait: An in vivo positron emission tomography study. Mov Disord [online serial]. John Wiley and Sons Inc.; 2014;29:1118–1124. Accessed at: /pmc/articles/PMC4162130/?report=abstract. Accessed September 17, 2020.

54. Horwitz B, Duara R, Rapoport SI. Intercorrelations of glucosemetabolic rates between brain regions: Application to healthy males in a state of reduced sensory input. J Cereb Blood Flow Metab [online serial]. J Cereb Blood Flow Metab; 1984;4:484–499. Accessed at: https://pubmed.ncbi.nlm.nih.gov/6501442/. Accessed August 25, 2020.

55. Lee DS, Kang H, Kim H, et al. Metabolic connectivity by interregional correlation analysis using statistical parametric mapping (SPM) and FDG brain PET; Methodological development and patterns of metabolic connectivity in adults. Eur J Nucl Med Mol Imaging [online serial]. Eur J Nucl Med Mol Imaging; 2008;35:1681–1691. Accessed at: https://pubmed.ncbi.nlm.nih.gov/18491089/. Accessed August 25, 2020.

56. Hahn A, Haeusler D, Kraus C, et al. Attenuated serotonin transporter association between dorsal raphe and ventral striatum in major depression. Hum Brain Mapp [online serial]. John Wiley and Sons Inc.; 2014;35:3857–3866. Accessed at: https://pubmed.ncbi.nlm.nih.gov/24443158/. Accessed August 25, 2020.

57. Verger A, Horowitz T, Chawki MB, et al. From metabolic connectivity to molecular connectivity: application to dopaminergic pathways. Eur J Nucl Med Mol Imaging [online serial]. Springer; 2020;47:413–424. Accessed at: https://doi.org/10.1007/s00259-019-04574-3. Accessed August 25, 2020.

58. Caminiti SP, Presotto L, Baroncini D, et al. Axonal damage and loss of connectivity in nigrostriatal and mesolimbic dopamine pathways in early Parkinson's disease. NeuroImage Clin [online serial]. Elsevier; 2017;14:734–740. Accessed at: http://dx.doi.org/10.1016/j.nicl.2017.03.011.

59. Gibb WRG, Lees AJ. The relevance of the Lewy body to the pathogenesis of idiopathic Parkinson's disease [online]. J. Neurol. Neurosurg. Psychiatry BMJ Publishing Group; 1988. p. 745–752. Accessed at: /pmc/articles/PMC1033142/?report=abstract. Accessed September 16, 2020.

60. Greuel A, Trezzi JP, Glaab E, et al. GBA Variants in Parkinson's Disease: Clinical, Metabolomic, and Multimodal Neuroimaging Phenotypes. Mov Disord. Epub 2020.:1–11.

61. Ruppert MC, Greuel A, Tahmasian M, et al. Network degeneration in Parkinson's disease: multimodal imaging of nigro-striato-cortical dysfunction. Brain [online serial]. NLM (Medline); 2020;143:944–959. Accessed at: https://pubmed.ncbi.nlm.nih.gov/32057084/. Accessed September 17, 2020.

62. Fahn, S. and Elton RL. Fahn, S. and Elton, R.L. (1987) Unified Parkinson's disease rating scale. In Fahn, S., Marsden, C.D., Calne, D. and Goldstein, M., Eds., Recent Developments in Parkinson's Disease, Macmillan Health Care Information, Florham Park, 153-163. Unified Park. Dis. Rat. scale 1987. p. 153–163.

63. Langston JW, Widner H, Goetz CG, et al. Core assessment program for intracerebral transplantations (CAPIT). Mov Disord [online serial]. John Wiley & Sons, Ltd; 1992;7:2–13. Accessed at: https://onlinelibrary.wiley.com/doi/full/10.1002/mds.870070103. Accessed September 17, 2020.

64. Tahmasian M, Eickhoff SB, Giehl K, et al. Resting-state functional reorganization in Parkinson's disease: An activation likelihood estimation meta-analysis [online]. Cortex Masson SpA; 2017. p. 119–138. Accessed at: https://pubmed.ncbi.nlm.nih.gov/28467917/. Accessed September 17, 2020.

65. Vogler A, Janssens J, Nyffeler T, Bohlhalter S, Vanbellingen T. German Translation and Validation of the "freezing of Gait Questionnaire" in Patients with Parkinson's Disease. Parkinsons Dis [online serial]. Hindawi Limited; 2015;2015. Accessed at: /pmc/articles/PMC4325214/?report=abstract. Accessed September 17, 2020.

66. Ruppert MC, Greuel A, Freigang J, et al. The default mode network and cognition in Parkinson's disease: A multimodal resting-state network approach. Hum Brain Mapp [online serial]. Hum Brain Mapp; Epub 2021 Feb 27.:hbm.25393. Accessed at: https://onlinelibrary.wiley.com/doi/10.1002/hbm.25393. Accessed March 7, 2021.

67. Folstein MF, Folstein SE, McHugh PR. "Mini-mental state". A practical method for grading the cognitive state of patients for the clinician. J Psychiatr Res [online serial]. J Psychiatr Res; 1975;12:189–198. Accessed at: https://pubmed.ncbi.nlm.nih.gov/1202204/. Accessed May 20, 2021.

68. Kalbe E, Calabrese P, Kohn N, et al. Screening for cognitive deficits in Parkinson's disease with the Parkinson neuropsychometric dementia assessment (PANDA) instrument. Park Relat Disord [online serial]. Parkinsonism Relat Disord; 2008;14:93–101. Accessed at: https://pubmed.ncbi.nlm.nih.gov/17707678/. Accessed September 17, 2020.

69. Beck, A. T., Steer, R. A., & Brown GK. Manual for the Beck Depression Inventory-II. Man. Beck Depress. Invent. San Antonio: TX: Psychological Corporation; 1996.

70. Peto V, Jenkinson C, Fitzpatrick R, Greenhall R. The Development and Validation of a Short Measure of Functioning and Well Being for Individuals with Parkinson ' s Disease Linked references are available on JSTOR for this article : The development and validation of a

short measure of functioning and wel. Qual Life Res. 1995;4:241–248.

71. García-Gómez FJ, García-Solís D, Luis-Simón FJ, et al. Elaboración de una plantilla de SPM para la normalización de imágenes de SPECT con 123I-Ioflupano. Rev Esp Med Nucl Imagen Mol [online serial]. Elsevier; 2013;32:350–356. Accessed at: https://www.elsevier.es/es-revista-revista-espanola-medicina-nuclear-e-125-articulo-elaboracion-una-plantilla-spm-normalizacion-S2253654X1300022X. Accessed April 8, 2021.

72. Kas A, Payoux P, Habert MO, et al. Validation of a standardized normalization template for statistical parametric mapping analysis of 123I-FP-CIT images. J Nucl Med [online serial]. J Nucl Med; 2007;48:1459–1467. Accessed at: https://pubmed.ncbi.nlm.nih.gov/17704252/. Accessed September 22, 2020.

73. Rolls ET, Huang CC, Lin CP, Feng J, Joliot M. Automated anatomical labelling atlas 3. Neuroimage. Academic Press Inc.; 2020;206:116189.

74. R Core Team. R: A Language and Environment for Statistical Computing [online]. R Foundation for Statistical Computing; 2021. Accessed at: https://www.r-project.org/.

75. Whitfield-Gabrieli S, Nieto-Castanon A. Conn: A Functional Connectivity Toolbox for Correlated and Anticorrelated Brain Networks. Brain Connect [online serial]. Brain Connect; 2012;2:125–141. Accessed at: https://pubmed.ncbi.nlm.nih.gov/22642651/. Accessed September 17, 2020.

76. Semkovska M, Quinlivan L, O'Grady T, et al. Cognitive function following a major depressive episode: a systematic review and meta-analysis. The Lancet Psychiatry [online serial]. Elsevier Ltd; 2019;6:851–861. Accessed at: http://www.thelancet.com/article/S2215036619302913/fulltext. Accessed March 10, 2021.

77. Allali G, Montembeault M, Brambati SM, et al. Brain structure covariance associated with gait control in aging. Journals Gerontol - Ser A Biol Sci Med Sci [online serial]. Oxford University Press; 2019;74:705–713. Accessed at: https://pubmed.ncbi.nlm.nih.gov/29846517/. Accessed January 31, 2021.

78. Ouchi Y. Changes in dopamine availability in the nigrostriatal and mesocortical dopaminergic systems by gait in Parkinson's disease. Brain [online serial]. 2001;124:784–792. Accessed at: https://academic.oup.com/brain/article-lookup/doi/10.1093/brain/124.4.784. Accessed January 16, 2020.

79. Robinson JL, Laird AR, Glahn DC, et al. The functional connectivity of the human caudate: An application of meta-analytic connectivity modeling with behavioral filtering. Neuroimage [online serial]. NIH Public Access; 2012;60:117–129. Accessed at: /pmc/articles/PMC3288226/?report=abstract. Accessed October 1, 2020.

80. Jarbo K, Verstynen TD. Converging structural and functional connectivity of orbitofrontal, dorsolateral prefrontal, and posterior parietal cortex in the human striatum. J Neurosci. 2015;35:3865–3878.

81. Seger CA. The visual corticostriatal loop through the tail of the caudate: Circuitry and function. Front Syst Neurosci. 2013;7:1–15.

82. Alves PN, Foulon C, Karolis V, et al. An improved neuroanatomical model of the default-mode network reconciles previous neuroimaging and neuropathological findings. Commun Biol [online serial]. Springer US; 2019;2:1–14. Accessed at: http://dx.doi.org/10.1038/s42003-019-0611-3.

83. Conio B, Martino M, Magioncalda P, et al. Opposite effects of dopamine and serotonin on

resting-state networks: review and implications for psychiatric disorders [online]. Mol. Psychiatry Springer Nature; 2020. p. 82–93. Accessed at: https://doi.org/10.1038/s41380-019-0406-4. Accessed October 1, 2020.

84. Cole DM, Beckmann CF, Oei NYL, Both S, van Gerven JMA, Rombouts SARB. Differential and distributed effects of dopamine neuromodulations on resting-state network connectivity. Neuroimage [online serial]. Neuroimage; 2013;78:59–67. Accessed at: https://pubmed.ncbi.nlm.nih.gov/23603346/. Accessed October 8, 2020.

85. Kelly C, De Zubicaray G, Di Martino A, et al. L-dopa modulates functional connectivity in striatal cognitive and motor networks: A double-blind placebo-controlled study. J Neurosci [online serial]. J Neurosci; 2009;29:7364–7378. Accessed at: https://pubmed.ncbi.nlm.nih.gov/19494158/. Accessed October 8, 2020.

86. Weele CMV, Siciliano CA, Tye KM. Dopamine tunes prefrontal outputs to orchestrate aversive processing. Brain Res. Elsevier B.V.; 2019. p. 16–31.

87. Salamone JD, Pardo M, Yohn SE, López-Cruz L, Sanmiguel N, Correa M. Mesolimbic dopamine and the regulation of motivated behavior. Curr Top Behav Neurosci. Springer Verlag; 2016;27:231–257.

88. Fasano A, Herzog J, Seifert E, Stolze H, Falk D, Volkmann J. Modulation of Gait Coordination by Subthalamic Stimulation Improves Freezing of Gait. 2011;26:844–851.

89. Fietzek UM, Zwosta J, Schroeteler FE, Ziegler K, Ceballos-Baumann AO. Levodopa changes the severity of freezing in Parkinson's disease. Park Relat Disord [online serial]. Parkinsonism Relat Disord; 2013;19:894–896. Accessed at: https://pubmed.ncbi.nlm.nih.gov/23642712/. Accessed October 8, 2020.

90. Lucas McKay J, Goldstein FC, Sommerfeld B, Bernhard D, Perez Parra S, Factor SA. Freezing of Gait can persist after an acute levodopa challenge in Parkinson's disease. npj Park Dis [online serial]. Springer US; 2019;5:1–8. Accessed at: http://dx.doi.org/10.1038/s41531-019-0099-z.

91. Amboni M, Stocchi F, Abbruzzese G, et al. Prevalence and associated features of self-reported freezing of gait in Parkinson disease: The DEEP FOG study. Park Relat Disord [online serial]. Elsevier Ltd; 2015;21:644–649. Accessed at: http://dx.doi.org/10.1016/j.parkreldis.2015.03.028.

92. Snijders AH, Takakusaki K, Debu B, et al. Physiology of freezing of gait. Ann Neurol. 2016;80:644–659.

93. Bohnen NI, Kanel P, Zhou Z, et al. Cholinergic system changes of falls and freezing of gait in Parkinson's disease. Ann Neurol [online serial]. John Wiley & Sons, Ltd; 2019;85:538–549. Accessed at: https://onlinelibrary.wiley.com/doi/abs/10.1002/ana.25430. Accessed October 1, 2020.

7. FIGURE LEGENDS

Figure. 1: Schematic representation of the workflow of molecular connectivity and resting-state functional connectivity analyses applied to FDOPA-PET scans and fMRI scans of FOG+ and FOG- patients in the current study. Initially, a group comparison of FDOPA-PET scans was performed between FOG+ and FOG- patients, which revealed more profound dopaminergic deficits in FOG+ patients. Seed regions of interest (ROIs) for subsequently performed functional connectivity analyses were placed based on the hypodopaminergic regions or represented atlas-based definitions of dopaminergic midbrain nuclei. Mean tracer uptake of regions constituting the mesocorticolimbic system (AALv3) was extracted from normalized FDOPA-PET scans and ROI-wise correlations were calculated between the seed ROI's tracer uptake and every other ROI to obtain covariant dopaminergic pathways. Resulting correlations were compared between FOG+ and FOG- patients by fisher's z test to evaluate impairments in dopaminergic pathway integrity in FOG. Significant differences in correlation coefficients were visualized by a connectogram. Similarly, mean BOLD time series were extracted from defined seed ROIs for each subject and voxel-wise correlations were examined and compared between both patient groups for the whole brain.

Figure 2 (A) Results of voxel-wise two-sample t-test of FDOPA-PET with the contrast FOG+<FOG- (p_{FWE}<0.05). FOG+ patients display lower dopamine metabolism in the left caudate nucleus. Coordinates in respective planes are displayed above. (B) Multiple boxplots with group comparisons of BP_d in the left caudate between FOG+ and FOG- patients in left- respectively right-lateralized individuals. * indicate significance at p< 0.05 in Welch's t-test. **(C)** Boxplot with group comparison of BP_d in the left caudate between left and right lateralized FOG+ patients.

Figure 3 Connectogram with atlas based ROIS (AALv3) of mesocortical and mesolimbic dopamine pathways with the bilateral ventral tegmental area as seed volume. Solely the significantly reduced interregional correlations in FOG+ compared to FOG- are displayed (p-values after FDR-correction for multiple testing). Differences in z-values after Fisher's z-test are indicated by color scale, lower values indicate higher impairment of connectivity in FOG+. Abbreviations: L/R: left/right, ACC: anterior cingulate cortex, ACC: anterior cingulate cortex, MCC: mid cingulate cortex, PCC; posterior cingulate cortex, HIP: hippocampus, PHG: parahippocampal gyrus, AMYG: amygdala, NAcc: nucleus accumbens, SFG: dorsolateral superior frontal gyrus, SFGmed: medial superior frontal gyrus, PFCventmed: ventromedial prefrontal gyrus, IFGorb: orbital inferior frontal gyrus, OFC: orbitofrontal cortex.

Figure 4 Results of rs-fMRI analysis with the applied contrast FOG+<FOG- (p_{FWE}<0.05). (A) Increased functional connectivity between left caudate nucleus and bilateral visual cortex, and (B)

increased functional connectivity between bilateral VTA and bilateral precuneus, bilateral superior lateral occipital cortex and right superior frontal gyrus was observed in freezers.

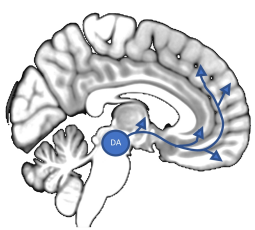

SEED SELECTION

FOG+ < FOG-

Atlas (AALv3)

Anatomical

[18F]-DOPA PET

Data-driven

SEED

[18F]-DOPA PET

SUBJECTS

EXTRACTION OF MEAN TRACER UPTAKE

SEED

Rs-fMRI

TIMESERIES

EXTRACTION OF MEAN BOLD TIMESERIES

AALv3

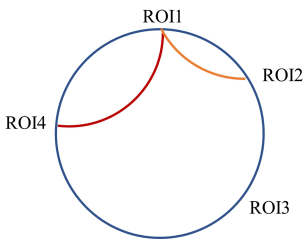

ROI-WISE CORRELATIONS

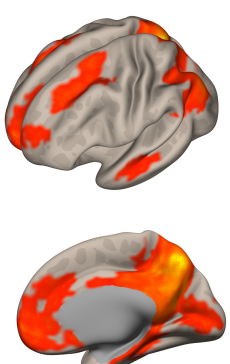

VOXEL-WISE CORRELATIONS

FOG+ < FOG-

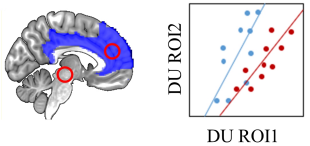

COMPARISON OF CORRELATIONS

FOG+ < FOG-

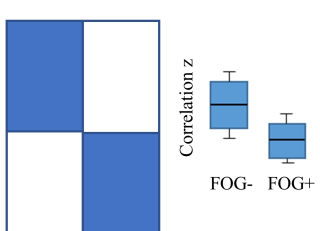

COMPARISON OF CORRELATIONS

Dopamine Depletion in Freezing of Gait (FOG+<FOG-)

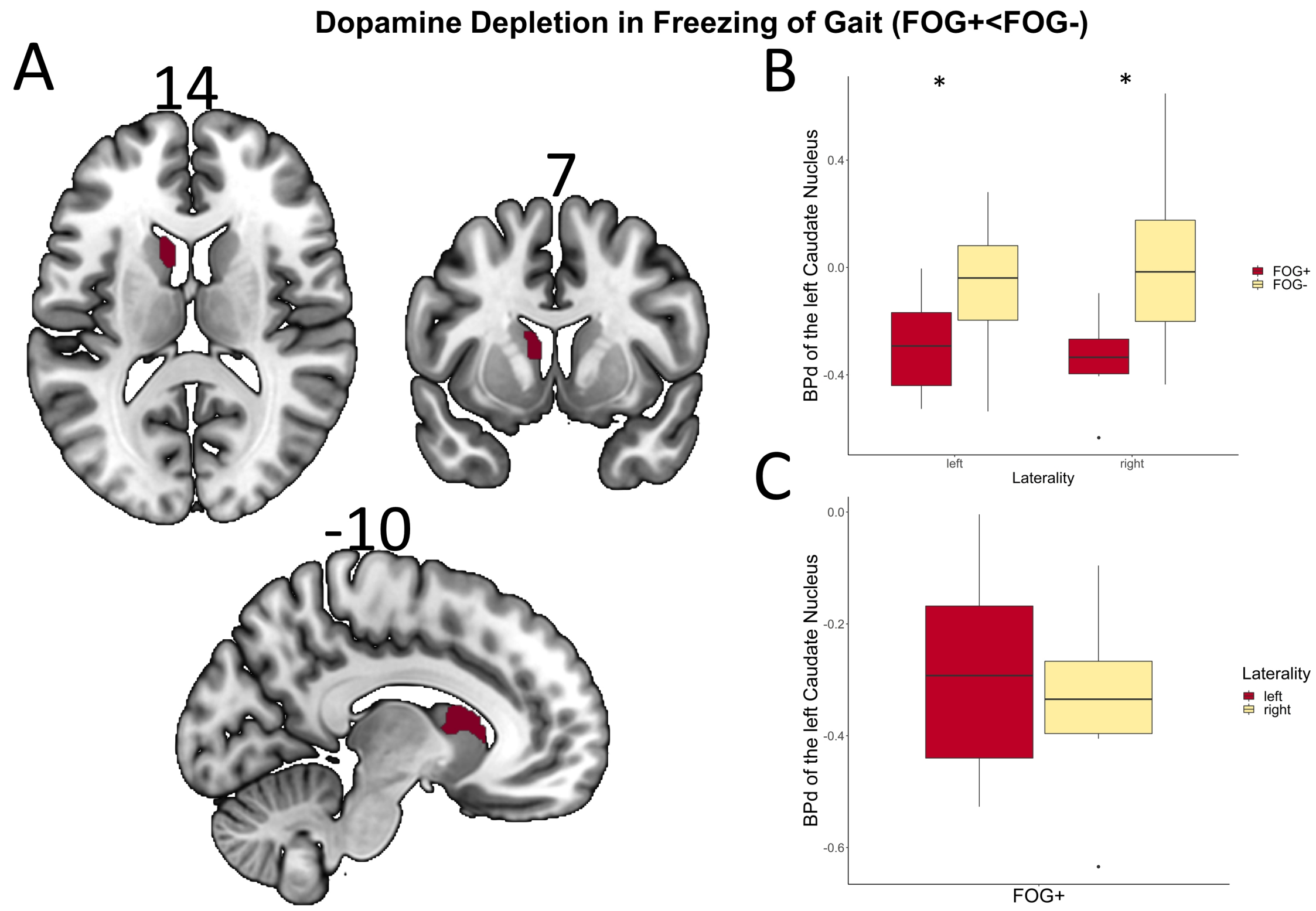

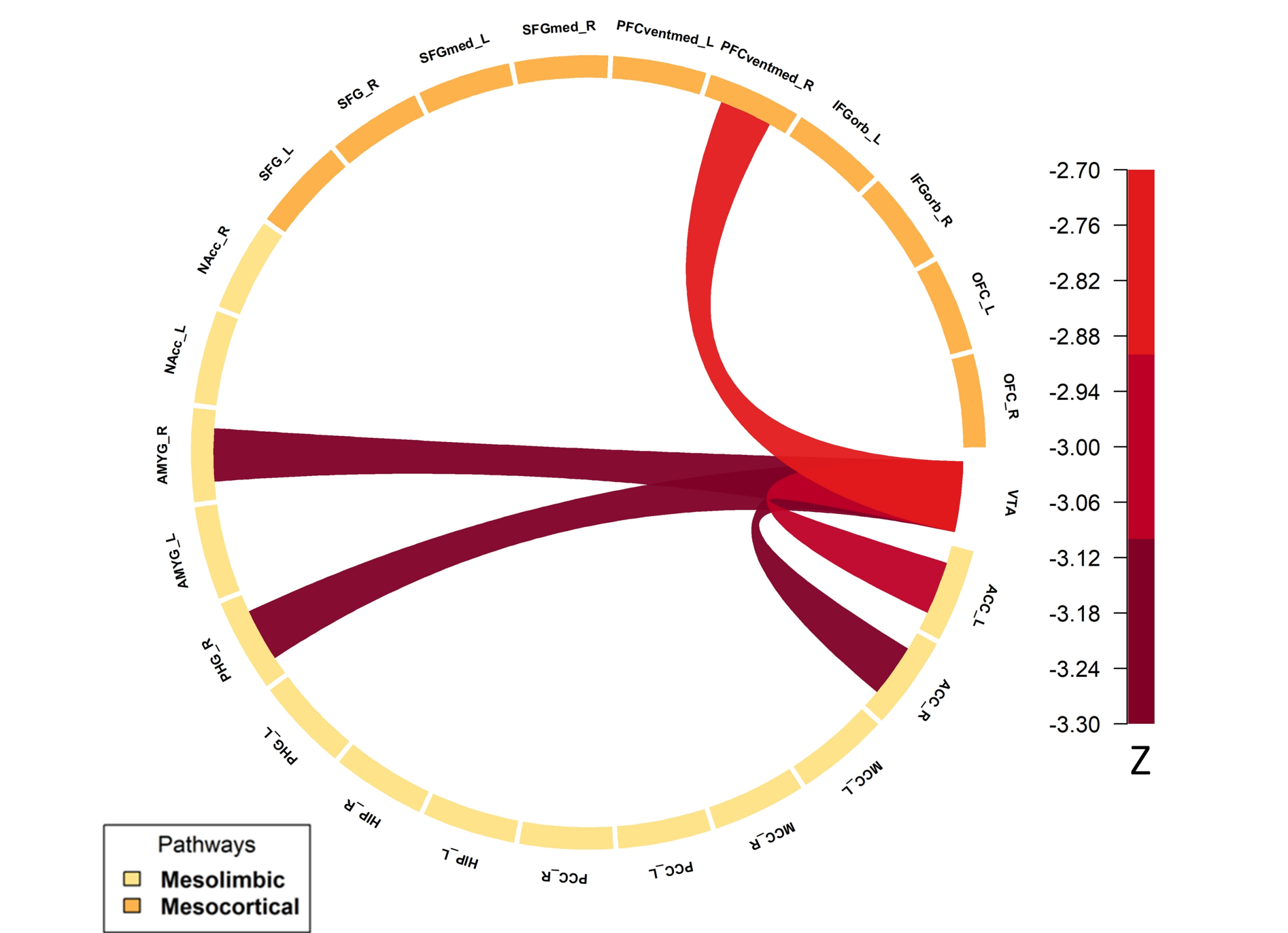
SFGmed_R
PFCventmed_L
PFCventmed_R
IFGorb_L
IFGorb_R
OFC_L
OFC_R
VTA
ACC_L
ACC_R
MCC_L
MCC_R
PCC_L
PCC_R
HIP_L
HIP_R
PHG_L
PHG_R
AMYG_L
AMYG_R
NAcc_L
NAcc_R
SFG_L
SFG_R
SFGmed_L
-2.70
-2.76
-2.82
-2.88
-2.94
-3.00
-3.06
-3.12
-3.18
-3.24
-3.30
Z
Pathways
Mesolimbic
Mesocortical

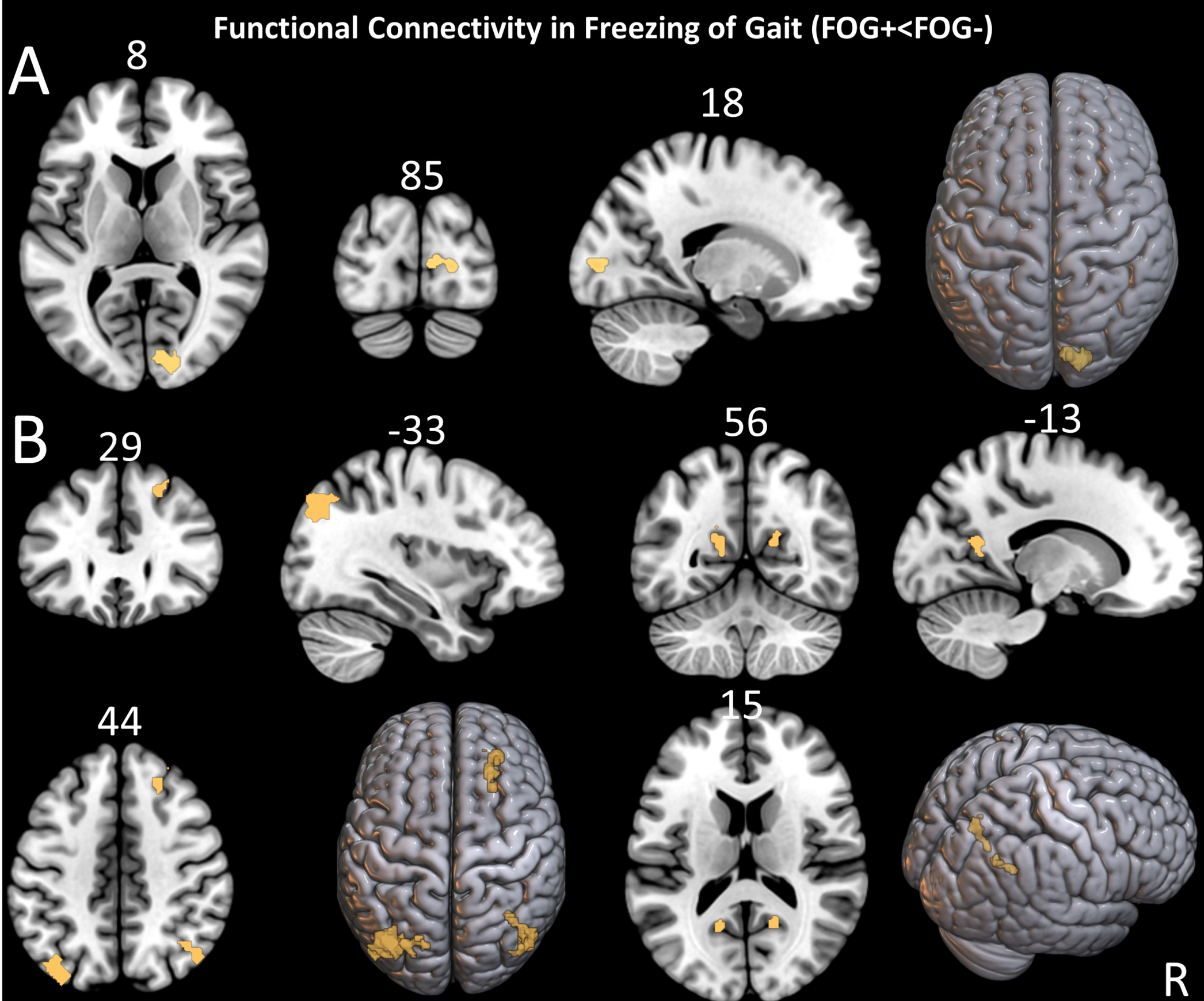
Functional Connectivity in Freezing of Gait (FOG+<FOG-)
A
8
85
18
B
29
-33
56
-13
44
15
R

Supplements:

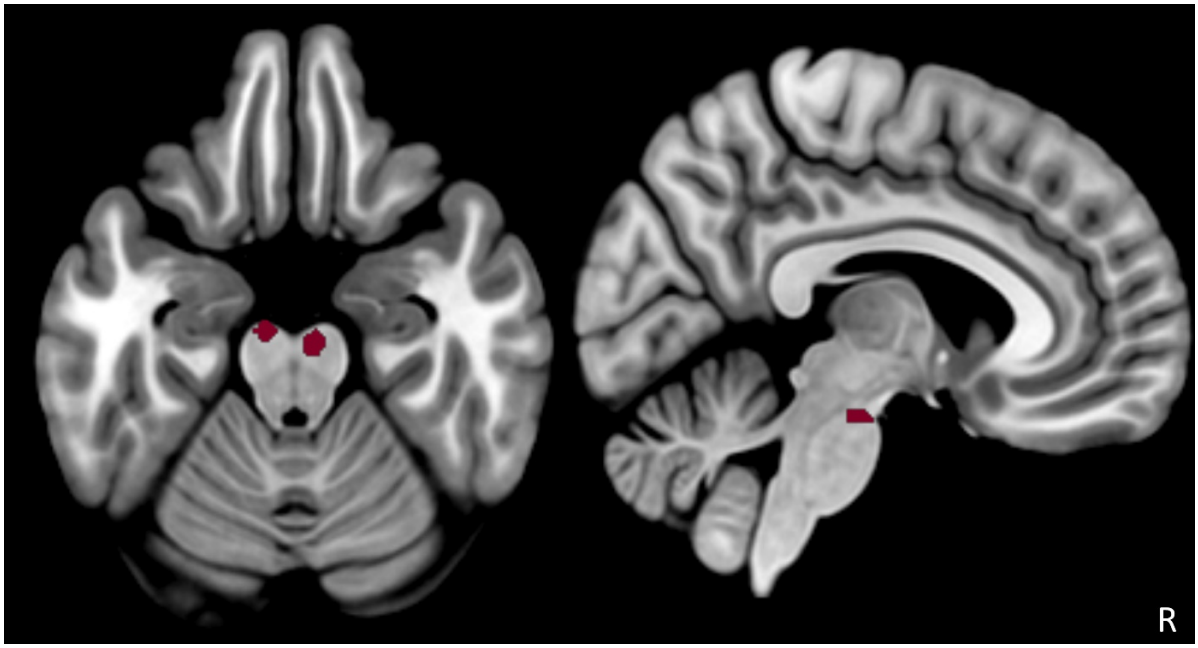

Supplementary Figure: Results of voxel-wise two-sample t-test of DOPA PET with the contrast FOG+<FOG- (uncorr p<0.001) with small volume correction for midbrain. The right cluster narrowly missed the FWE threshold and overlapped with the VTA altas ROI from AAL (MNI 4/-20/-22, T= 3.83, k=18, p_{FWE}=0.085, p_{uncorr}<0.001). The smaller left cluster was located more ventrally and was not unanimously assignable to a specific midbrain nucleus (MNI -8/-16/-22, T=3.54, k=10, p_{FWE}=0.108, p_{uncorr}=0.001).

Supplementary Table 1: Demographic and Clinical Data FDOPA subgroup

	FOG+ n = 21	FOG- n = 23	p-value	Test statistic
Age [years]	68.4	66.2	0.388	t=0.87
Sex m/f	13/8	14/9	0.944	X^2=0.01
Laterality (right/left/equal)	6/14/1	11/10/2	0.304	X^2=2.38
Disease duration [years]	4.9 ± 3.6	4.3 ± 3.2	0.731	W=256.5
FOG-severity	10.6 ± 4.7	2.2 ± 1.6	< 0.001	W=479.5
UPDRS-III	27.6 ± 9.2	22.4 ± 7.4	0.130	W=306.0
PGS	2.9 ± 2.0	1.3 ± 1.5	0.005	W=360.5
BDI-II	10.6 ± 4.7	8.7 ± 7.0	0.087	W=314.5
PDQ39	23.8 ± 11.1	20.5 ± 19.7	0.060	W=322.0
Hoehn & Yahr	2.4 ± 0.4	2.4 ± 0.4	0.213	W=289.5
LEDD [mg]	485 ± 289	422 ± 236	0.285	W=287.5
Levodopa response	0.3 ± 0.1	0.3 ± 0.1	0.552	t=-0.57
Neuropsychological Data FDOPA subgroup				
MMST	28.8 ± 1.1	28.0 ± 2.3	0.535	W=267.5
PANDA	24.1 ± 4.5	22.2 ± 5.6	0.305	W=285.5
executive Z-score	-0.06 ± 0.6	-0.21 ± 0.6	0.689	W=259.0
memory Z-score	-0.22 ± 1.2	-0.52 ± 1.2	0.246	W=291.0
attention Z-score	-0.18 ± 0.79	-0.29 ± 0.72	0.715	t=-0.49
language Z-score	0.41 ± 0.67	0.15 ± 0.65	0.086	W=315.0
visuo-spatial Z-score	0.03 ± 0.9	-0.73 ± 1.2	0.032	W=331.0
global cognition Z-score	-0.02 ± 0.46	-0.34 ± 0.5	0.026	W=337.0

Numeric variables are shown as mean ± standard deviation. Group comparisons were calculated using Welch's t-test or Wilcoxon-test. Nominal variables were compared by Chi-squared test. Levodopa response is defined as ratio of UPDRS in OFF and ON state. Abbreviations: LEDD: Levodopa equivalent daily dose, PDQ39: Parkinson's Disease Questionnaire 39, PANDA: Parkinson's Neuropsychometric Dementia Assessment, MMST: Mini-Mental Status Examination, UPDRS: Unified Parkinson's Disease Rating Scale, PGS: Postural-Gait-Score

Supplementary Table 2: Masks for small volume correction

Masks	AAL v3 Regions
Striatum / Nigrostriatal	Caudate_R, Caudate_L, Striatum_R, Striatum_L, Pallidum_L, Pallidum_R
Mesolimbic	Hippocampus_R, Hippocampus_L, ParaHippocampal_R, ParaHippocampal_L, Amygdala_R, Amygdala_L, Cingulum_Ant_ R, Cingulum_Ant_ L, Cingulum_Mid_ R, Cingulum_Mid_ L, Cingulum_Post_ R,Cingulum_Post_L, NAcc_L, NAcc_R
Mesocortical	Frontal_Sup_R, Frontal_Sup_L, Frontal_Sup_Medial_R, Frontal_Sup_Medial_L, Frontal_Sup_Orb_R, Frontal_Sup_Orb_L, Frontal_Mid_Orb_R, Frontal_Mid_Orb_R, OFC_R, OFC_L (OFCmed, OFCant, OFCpost, OFClat)